Free nanoscale sodium clusters studied by core-level photoelectron spectroscopy

S. Peredkov,[1,*] G. Öhrwall,[2] J. Schulz,[3] M. Lundwall,[2] T. Rander,[2] A. Lindblad,[2] H. Bergersen,[2] A. Rosso,[2] W. Pokapanich,[2] N. Mårtensson,[4,2] S. Svensson,[2] S. L. Sorensen,[1] O. Björneholm,[2] and M. Tchaplyguine[4]

[1]*Department of Synchrotron Radiation Research, Lund University, Box-118, SE-22100 Lund, Sweden*

[2]*Department of Physics, Uppsala University, Box 530, SE-75121 Uppsala, Sweden*

[3]*Department of Physical Sciences, University of Oulu, Box 3000, FIN-90014 Oulu, Finland*

[4]*Max-lab, Lund University, Box 118, SE-22100 Lund, Sweden*

(Received 22 January 2007; revised manuscript received 25 March 2007; published 6 June 2007)

Free sodium metal clusters have been studied by probing the Na $2p$ core level using x-ray photoelectron spectroscopy (XPS) and Auger electron spectroscopy (AES). The development of electronic structure with size has been studied and discussed in comparison with the atom, dimer, and solid. Information on cluster metallic properties, size, and temperature has been deduced from the XPS measurements. For the large $\langle N \rangle > 10^3$ Na clusters, the surface and bulk sites have been separated in the photoelectron signal. Auger spectra allowed extracting the information on the valence band. The present study introduces *core-level* spectroscopies XPS and AES into the field of *free neutral metal* cluster research.

DOI: 10.1103/PhysRevB.75.235407 PACS number(s): 61.46.−w, 61.46.Bc, 36.40.−c, 79.60.−i

I. INTRODUCTION

The primary goal of cluster science is to follow the evolution of geometric and electronic structure as a function of cluster size.[1] The electronic structure changes drastically with size, from localized atomic orbitals over molecularlike orbitals for small clusters to bandlike states for large clusters approaching the infinite solid. The study of *free* clusters is crucial to fully understand the microscopic origin of the size-dependent properties. A particularly challenging area concerns clusters of metal atoms. Size-dependent studies of metal clusters can illuminate the development of the fundamental properties of metals, first of all, conductivity.[2]

Core-level spectroscopy, especially combined with synchrotron radiation, has proven to be a valuable tool in the study of the electronic and geometric structures of isolated atoms, molecules, surfaces, and solids. The techniques include x-ray photoelectron spectroscopy (XPS), x-ray absorption spectroscopy (XAS), and Auger electron spectroscopy (AES). Many size-dependent properties of clusters are related to the large fraction of low-coordination atoms at the cluster surface, and core-level spectroscopy is a method that can separate surface and bulk responses. Due to the atomic character of the core orbitals, core-level spectroscopy probes the local surrounding of the core-hole site. Studies of free clusters using synchrotron-radiation-based core-level spectroscopies have been performed on pure and mixed rare-gas and molecular clusters.[3–7] It is, for instance, possible to separate surface and bulk spectral features and even different types of surface sites.[8,9] For mixed rare-gas clusters, information about radial structuring and layering has been obtained by XPS,[6,10] and AES studies have revealed interesting aspects of the charge delocalization in water.[7] Similar core-level spectroscopy studies of free metal clusters have been difficult to carry out mainly due to the insufficient sample density. A number of works on *supported* clusters have been carried out. However, the inherent properties of clusters are, to a great extent, distorted and obscured by the changes imposed on their geometry and energy structure by the growth or deposition procedure and by the influence of the substrate.[11] In supported clusters, the changes due to the external factors are difficult to distinguish from those caused by the cluster size or structure variation. Only very recently, the first such core-level spectroscopy study of free metal clusters, XAS of titanium clusters, was presented.[12]

In the present work, sodium has been chosen as a parent material for free metal clusters. Solid sodium is often regarded as a "perfect" free-electron metal.[13] Free sodium atoms and solid multilayers have been studied by means of synchrotron-based x-ray photoelectron spectroscopy.[14,15] The present study introduces *core-level* spectroscopies XPS and AES into the field of *free neutral metallic* cluster studies. The development of electronic and geometric structures with size is made evident by comparison of the present cluster data with earlier results reported for the atom, dimer, and solid.[14,16,17] The well-established model for the size dependence of the ionization potential, representing ionization of a delocalized electron at the Fermi level, is extended to the case of ionization of localized core levels. For all Na clusters in the present work, the surface and bulk sites have been separated in the photoelectron signal. Information on cluster metallicity, size, and temperature has been deduced from the XPS measurements. Auger spectra have been shown to contain important energy characteristics, such as the cluster work function and the valence-band width.

These results demonstrate the potential of core-level spectroscopies such as XPS and AES to provide valuable data on free metal clusters.

II. EXPERIMENT

To produce clusters of sodium, a gas-aggregation source similar to that in Refs. 18–20 has been used. In such a setup, a source of metal vapor—an oven with solid sodium—is placed into a liquid-nitrogen-cooled cryostat through which an inert gas (He and Ar) at the pressure of a few millibars flows. Metal atoms are vaporized into the flow of the cold carrier gas where condensation occurs as the result of super-

saturation. The temperature of the sodium oven could be raised up to 600 K producing partial vapor pressures of 0.5 mbar. The carrier gas flow transfers the metal clusters through a narrow 30-mm-long nozzle to the ionization chamber. The Laval-shaped nozzle has a 1 mm entrance diameter and a channel diameter of 2.5 mm. The oven is covered with a thermal shield consisting of several insulating ceramic and metal layers. More details of the experimental setup and the gas-aggregation source are given in our paper devoted to the magnetron-based metal vapor source.[21] In the present case, the sodium oven replaced the magnetron sputtering gun inside the cryostat. Optimal conditions for producing large clusters were obtained by operating the cryostat at cryogenic temperatures while the oven was run at the highest heating power compatible with the liquid-nitrogen cooling capacity in order to maintain stable clustering conditions.

Early studies of large sodium clusters with $\langle N \rangle \approx 10^4$ showed that higher carrier gas pressures and a higher fraction of Ar in the He-Ar mixture lead to larger average cluster sizes.[18] We have implemented the same strategy, with similar pressures for the Ar/He mixture (30% Ar and 70% He) or with pure argon. The cryostat exit nozzle geometry was also similar to that of Ref. 18. This is expected to result in sodium clusters containing several tens of thousands of atoms. By varying the cryostat temperature and changing the gas composition, we could influence the cluster size. Pure argon, along with the lowest possible cryostat temperature, was expected to give the largest cluster size.

All measurements were performed at the soft-x-ray undulator beamline I411 at Max-lab synchrotron radiation facility (Lund, Sweden).[22] This beamline has a photon energy range of 60–1500 eV and is equipped with a rotatable Scienta R4000 electrostatic electron energy analyzer fixed in the present experiments at 90° to the horizontal polarization plane of the synchrotron radiation.

The Na $2p$ core-level XPS spectra were measured at several photon energies in the range from 60 to $\approx$200 eV. The spectrum in Fig. 1 was recorded at 74 eV photon energy. Such a choice made it possible to utilize the properties of the I411 beamline radiation in an optimal way: it provided the highest ionization cross section for the core-level under investigation and the highest photon resolution in the region where the photon flux is close to maximum. The total experimental resolution in the XPS spectra defined by the monochromator and the electron energy analyzer varied between 40 and 85 meV depending on the settings. Normal Auger spectra generated as the result of the $2p$ level electronic decay were recorded at photon energies of 81 and 90 eV with the spectrometer resolution of 125 meV.

The absolute energy scale was calibrated in each XPS spectrum using several argon $3p4nl$ satellite lines appearing due to the presence of the carrier gas in the ionization volume: $(^3P)3d(^2D_{5/2})$ at 34.50 eV, $(^3P)3d(^2D_{3/2})$ at 34.42 eV, and $(^1D)3s(^2D_{5/2})$ at 34.21 eV.[23] In most of the spectra presented below, the argon lines have been subtracted. Auger spectra were calibrated using $3s^13p^5nl$ argon satellite lines at 50.4 and 51.36 eV binding energies[23] (not included in the presented spectrum). The energy scales are referred to the vacuum level.

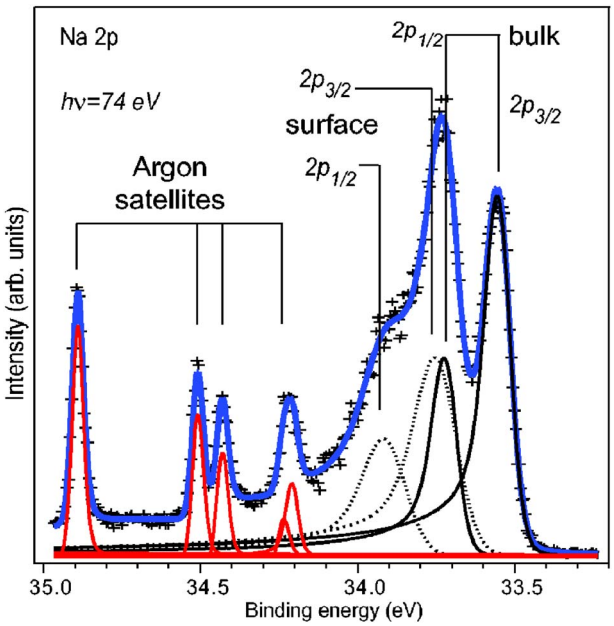

FIG. 1. (Color online) High-resolution sodium $2p$ XPS spectrum of large $\langle N \rangle \approx 10^4$–$10^6$ clusters measured at $h\nu$=74 eV (crosses). The spectrum is fitted assuming bulk (solid line) and surface (dotted line) features for each of the $2p_{3/2}$ and $2p_{1/2}$ spin-orbit components. The total resolution is estimated to be around 40 meV.

III. RESULTS

A. XPS results

A typical Na $2p$ photoelectron spectrum for the clusters our source produces is presented in Fig. 1. The spectral interval in Fig. 1 also contains the above-mentioned argon satellite lines. The spectral pattern is almost identical to that of the solid Na.[15] Such a resemblance has also been observed for the XPS spectra of the free large atomic and molecular clusters. We interpret the main spectral features in the same terms as in Ref. 15: each of the two spin-orbit components has two peaks—one due to the bulk and the other due to the surface atoms of the cluster. The well resolved peak at 33.55 eV is the bulk $2p_{3/2}$ component placing the bulk $2p_{1/2}$ peak at $\approx$33.72 eV. This latter peak overlaps with the surface $2p_{1/2}$ component at $\approx$33.93 eV, resulting in three main features in the cluster spectrum.

In the fitting procedure, the intensity ratio of the $2p_{1/2}$ to $2p_{3/2}$ feature has been taken to be equal to 0.5. The initial guesses for the peak parameters, such as the spin-orbit splitting, the bulk-surface separation, and the Lorentzian core-hole lifetime determined width, have been taken equal to the solid feature values.[15] The lifetime width of 10 meV has been assumed for both the bulk and the surface lines. The close resemblance of the cluster and solid spectra has also determined the choice of the Doniach-Šunjić[24] spectral function for fitting the experimental curves, implying the clusters to be metallic. For the bulk-metal XPS, the Doniach-Šunjić line shape is a spectral profile appearing due to the valence electrons being excited across the Fermi level into the empty conduction band, which leads to a continuous asymmetric tail toward lower binding energy in the XPS spectrum. The

Gaussian width of the features represents the broadening due to the experimental instrument function and due to the thermal vibrations.[15] *A priori*, one should assume that the cluster-size distribution also contributes to the Gaussian width.[25] In the present case, however, the closeness of the experimental cluster widths to those of the solid indicates an insignificant size effect. The fitting of the spectra has been done after the subtraction of the background, which has been approximated by a cubic polynomial.

The fit produces Doniach-Šunjić profile singularity indices, defining the asymmetry of the spectral shape, very close to those reported for solid sodium:[17] $a_b=0.18\pm0.01$ for the bulk and $a_s=0.21\pm0.01$ for the surface.

Although a significant fraction of the linewidth in the XPS spectrum in Fig. 1 is the instrumental broadening ($\approx$40 meV), the cluster temperature plays a noticeable role in the measured width. For the spectrum in Fig. 1, the Gaussian widths due to the phonon broadening of 85 ± 2 meV for the bulk and 142 ± 2 meV for the surface have been extracted. Riffe *et al.*[15] studied the temperature dependence of the linewidth of the $2p$ components of solid sodium, where they observed a much stronger response of the surface component width to the sample heating. The results were explained by the presence of a surface-specific relaxation channel through the normal-to-surface vibrations (phonon broadening) opened for the surface-atom core ionization. Using the data from the study,[15] it is possible to estimate the cluster temperature which is otherwise nontrivial to determine. Indeed, in a gas-aggregation source, only a part of the oven power is used to vaporize the metal; the excess energy heats up the carrier gas. The beam then undergoes an expansion which further cools the clusters. Thus, the cluster temperature can be significantly different from the cryostat temperature.

From the Gaussian width values (85 meV for the bulk and 142 meV for the surface) using the results of Ref. 15, we obtain an estimate of the cluster temperature of $\approx$130 K—close to the cryostat nozzle temperature of $\approx$100 K and to the cryostat body T of $\approx$135 K. Thus, we conclude that the particles are efficiently thermalized in the source. In principle, such a temperature determination procedure can be applied to free clusters, in general, when the XPS results for the solid are known.

As was mentioned above, the 74 eV photon energy at which the spectrum in Fig. 1 was recorded allowed using the properties of the radiation and the cross section in a nearly optimal way. A set of core-level cluster spectra recorded at several, higher photon energies can shed light on the cluster size and on the internal electron-scattering characteristics, such as an effective electron attenuation length.[5] The spectra recorded at three different photon energies—74, 120, and 198 eV—are presented in Fig. 2.

The electron attenuation length in solids is sensitive to the kinetic energy of electrons. In the range of electron kinetic energies from 40 to 200 eV in solid sodium, the electron attenuation length increases nearly linearly from 4 to 14 Å.[26] The photoelectrons from the low-energy part of this range are inelastically scattered in the cluster interior and contribute mainly to the signal from the cluster surface. Higher-energy photoelectrons are much less attenuated. Thus, varying the energy of the ionizing photons, one can emphasize the contribution from the surface or from the bulk of a cluster.

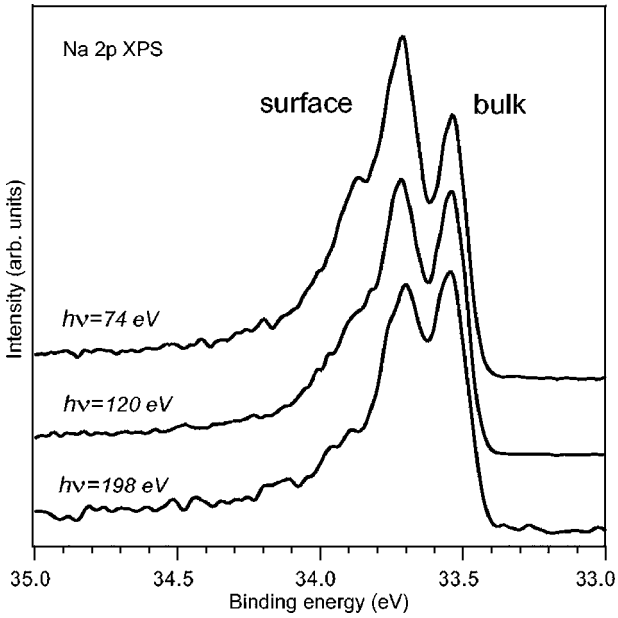

FIG. 2. $2p$ XPS spectra of large $\langle N\rangle\approx10^4-10^6$ sodium clusters measured at three different photon energies: 74, 120, and 198 eV. Argon lines have been subtracted from the cluster signal. All spectra are normalized to the height of the $2p_{3/2}$ bulk signal. The instrumental resolution is 85 meV.

In the series of measurements (Fig. 2) at the same clustering conditions, the relative intensity of the bulk signal is lowest at 74 eV with the bulk-to-surface intensity (area) ratio of $I_b/I_s\approx0.9$. At higher photon energies, the signal from the surface site becomes relatively weaker: the bulk-to-surface ratio changes from 1.4 to 3.0 as the photon energy is tuned from 120 to 198 eV.

The existing methods for the cluster-size estimation using bulk-to-surface ratios extracted from the XPS spectra[5,27] work better for small clusters ($\langle N\rangle\leqslant1000$). In the present work, clusters of a much larger size are produced. We will return to this subject in more detail below and the estimation of the cluster sizes will be attempted.

In the present work, we also aim to determine the change of the binding energy with cluster size. In Fig. 3, we present spectra for the two currently available, stable clustering conditions expected to produce the largest and the smallest clusters. These cluster spectra were recorded at 74 and 120 eV photon energies. The spectrum recorded with "smaller size conditions" was obtained with the Ar-He mixture at a cryostat temperature (measured at the nozzle) of 100 K, and with the oven at 520 K. The spectrum for "larger size conditions" was recorded with pure argon and with the oven at 560 K temperature. The cryostat was held at a temperature of 100 K. As can be seen from Fig. 2, both the binding energies of the cluster peaks and the surface-to-bulk ratio differ in the spectra recorded at the two different conditions. We attribute it to the change of the cluster size.

In the spectra recorded at 74 eV photon energy [Fig. 2(a)], the smaller clusters have the bulk-to-surface ratio

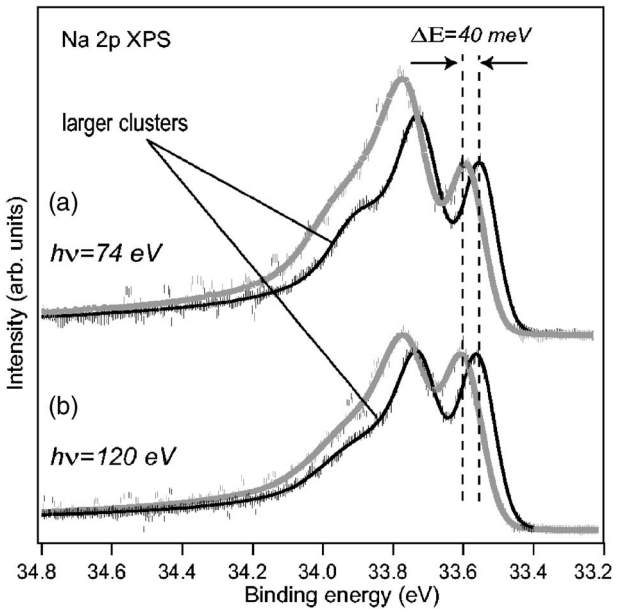

FIG. 3. Photoelectron spectra for two different sizes of sodium clusters measured at photon energies of (a) 74 eV and (b) 120 eV. The smaller cluster spectra (gray line) are shifted relative to the larger cluster spectra (black line) toward higher binding energies by ≈40 meV. All spectra are normalized to the height of the $2p_{3/2}$ bulk signal.

I_b/I_s(small)=0.7, and the larger clusters have I_b/I_s(large) =0.9. In the 120 eV spectra, I_b/I_s(small)=1.0, and I_b/I_s(large)=1.4. The lower bulk-to-surface ratio is consistent with the smaller clusters in the case of smaller size conditions.

This size difference is also manifested as a binding-energy shift. The precise energy calibration to the argon satellite lines in the spectra (subtracted here) allowed the determination of an absolute 40 meV shift between the $2p_{3/2}$ bulk peak positions: this peak recorded at smaller size conditions is shifted, as expected, toward higher binding energies relative to the larger size conditions.

B. Normal Auger spectra

The pathway of the Na $2p$ core-hole decay changes from the atom to the cluster. In the atomic case, the presence of only one valence electron excludes the normal Auger (NA) decay possibility, leaving the slow fluorescence as the only decay mechanism. Auger decay becomes possible in the sodium dimer[16] where the $3s$-derived molecular orbital contains two electrons. The resulting final state has no bonding valence electrons. The spectral shape of the dimer Auger feature is governed by the purely repulsive nature of the final state, resulting in an ≈1 eV wide, Gaussian-like peak.[16] The normal Auger spectrum of large clusters recorded at 90 eV photon energy in the present work is shown in Fig. 4. Another ionization energy (81 eV) gave the same kinetic-energy positions and spectral shapes, confirming the origin of the feature as due to the normal Auger decay. In contrast to the 0.7 eV wide dimer Auger spectrum, the cluster feature

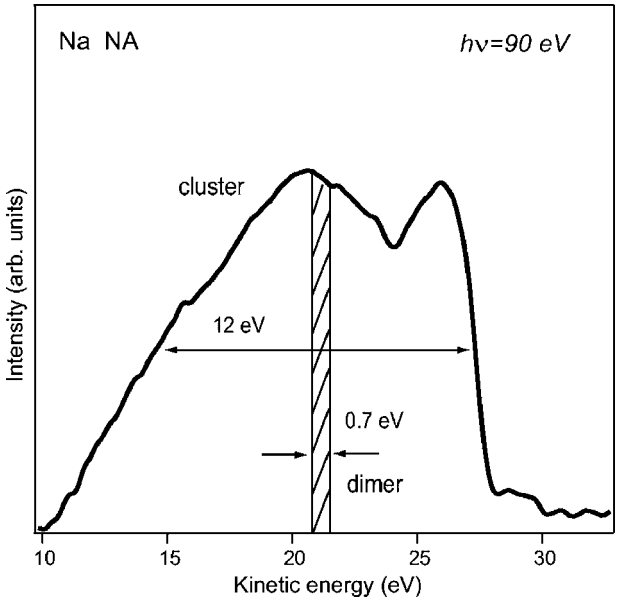

FIG. 4. Normal Auger spectrum of sodium clusters recorded using 90 eV photon energy. Dimer Auger feature width and position are also shown.

spans a ≈12 eV interval measured at half maximum (Fig. 4) from 27.5 to 15 eV. For comparison, the energy position and width of a dimer Auger spectrum is also shown in Fig. 4.

IV. DISCUSSION

A. Atom, dimer, and large cluster XPS comparison

The XPS spectra of the Na atoms,[14] dimers,[16] and large clusters are compared in Fig. 5. As the figure illustrates, the XPS spectra exhibit substantial changes with the number of atoms.

The atomic XPS spectrum consists of a group of lines, which are due to the different energy levels of the final

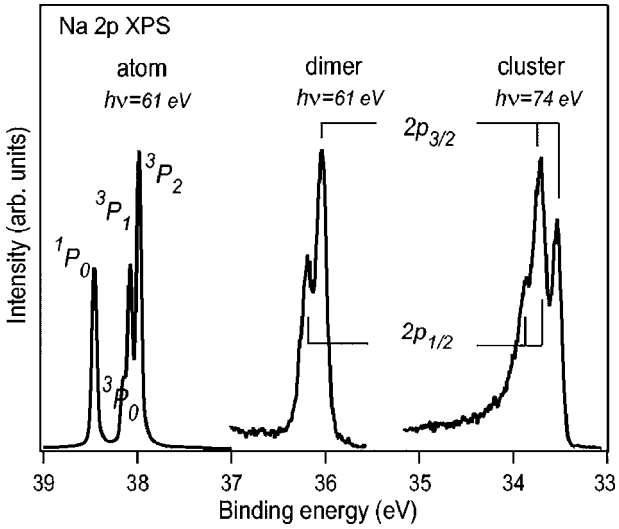

FIG. 5. Comparison of atomic (Ref. 14), dimer (Ref. 16), and sodium cluster $2p$ XPS spectra.

$2p^{-1}3s$ state configuration, where the two open shells ($2p$ and $3s$) couple. The dimer binding energy is ≈2 eV lower than the $^3P_2$ atomic level. This dramatic shift is due to both initial- and final-state effects in dimers.[16] The formation of a molecular σ_g orbital from the two atomic $3s$ orbitals alters the initial-state energy. In the final state, the screening of the $2p$ hole by the electrons in this delocalized σ_g molecular orbital takes place. The line shape in the dimer is also altered. The dimer spectrum consists of two peaks, which resemble the spin-orbit-split components observed for solid Na. The completely filled g orbital has no multiplets, so the $2p$ state contains the only uncoupled electron. The individual spin-orbit dimer spectral components also contain unresolved vibrational structure.[16]

The binding energy of the $2p$ levels in the cluster is about 4.4 eV lower than for the atom. This energy shift is calculated as the difference between the lowest in energy $^3P_2$ atomic line and $2p_{3/2}$ cluster bulk peak positions. This shift is also a reflection of both initial- and final-state effects. The initial state is altered by the formation of a filled $3s$ band, which also contains contributions from the unfilled $3p$ levels. In the final state, the site from which the $2p$ core electron is ejected becomes screened by delocalized valence-band electrons. The degree of screening is governed by the mobility of free electrons. In metals and large metallic clusters, a core hole will be completely screened. Small clusters may have a discrete valence-band structure. At a certain size, they can have semiconductorlike valence and conduction bands which are not merged. The limited mobility of the electrons in a discrete band structure leads to incomplete screening. Thus, the binding-energy shift is a measure of metallicity in clusters.

As discussed above, the shape of the large cluster $2p$-ionization spectrum is due to two spin-orbit-split components. The absence of multiplet splitting is understood as a weakened coupling between the $2p$ hole and the $3s$ electrons due to the delocalization of these band electrons. The line shape also differs remarkably from the atomic and dimer spectra—as mentioned above, it is strongly asymmetric toward higher binding energy due to the metallic electronic structure.

The comparison of atom, dimer, and cluster spectra demonstrates the sensitivity of the XPS method to the system size. Another important quantity which can be accurately measured using XPS is the absolute ionization energy, which allows estimating the size of the clusters.

B. Cluster-size estimation from the core-level binding energy

For the case of valence ionization, the dependence of the ionization potential (or work function), i.e., the binding energy of the states at the Fermi level $E_{Fermi}(R)$, on the size of metal clusters has been studied extensively.[28–30] A large metal cluster can be well approximated with a conducting sphere,[29] so that the work function of such a cluster differs from the work function of planar solid by a term defined largely by classical electrostatics. Just as for a macroscopic metal sphere, the positively charged hole is delocalized over the cluster surface. The smaller the clusters are, the smaller the area for the charge delocalization is. This results in an increase in the binding energy with decreasing size. For a given radius R of the initially neutral cluster, its ionization energy $E_{cl}(R)$ is described by the following formula (if the classical description is chosen, Ref. 28):

$$E_{cl}(R) = E_\infty + \Delta E(Z,R) = E_\infty + \left(Z + \frac{1}{2}\right)\frac{e^2}{R}, \tag{1}$$

where E_∞ is the work function of the planar bulk and Z is the initial cluster charge. For the present case, $Z=0$,

$$E_{cl}(R) = E_\infty + \frac{7.2}{R(\text{Å})}\ (\text{eV}). \tag{2}$$

Earlier experimental studies (for example, Refs. 28 and 30) of the *valence* binding-energy size dependence confirmed this model for large metal clusters, but deviations are observed for small sizes. Such deviations signify changes in electronic and geometric structures, as exemplified by the size-induced metal-insulator transition in Hg clusters connected to a transition from van der Waals to metallic bonding.[30]

Equations (1) and (2) describe the situation when an electron is emitted from a delocalized valence band, where the electrons and holes move freely. The resulting electric field outside the charged sphere is $E=Q/R^2$, where $Q=+1$ is the sum of charges on a sphere and R is the sphere radius. In a *core* ionization process, a *localized* positive charge (core hole) is created. This positive charge remains on the atomic site—at least until the Auger process sets in and the core hole is filled. Such a localized positive charge in a metallic cluster causes a rearrangement of the electron density in the cluster, resulting in a complete screening. The free-electron motion proceeds until the potential over the sphere volume is uniform. The positively charged hole is delocalized over the cluster surface. This leads to a spherically symmetric electric field outside the sphere. According to Gauss' theorem, the electric field will have the same value as above since the total charge of the sphere is the same as in the case of the valence ionization. Thus, we can apply the above formalism to both valence and core ionized clusters.

A rough estimate of the cluster dimension for spherical clusters with 10^4 atoms and an intershell separation of 2.48 Å is several nanometers.[31] [The separation is taken equal to the interplanar distance in a solid sodium bcc crystal in the (111) direction]. For clusters with 10^5 atoms, the cluster radius doubles. This radius increase implies a change in the deviation of the bulk ionization potential from the planar solid value [Eq. (2)] from 0.2 to 0.09 eV. For a cluster with 10^6 atoms, the estimated deviation is 0.04 eV from the planar solid ionization potential. The knowledge of the absolute value of the cluster ionization potential, on the one hand, and for the infinite solid, on the other hand, enables the use of Eq. (2) to estimate the cluster size.

For free particles such as atoms, molecules, and clusters, binding energies are commonly referenced to the vacuum level, denoted below as E_{vacuum}. For solid metals, however, binding energies E_{solid} are instead usually given with the

TABLE I. Estimation of cluster sizes from the $2p$ binding energy of sodium clusters and solid calculated using shell model and/or bulk density.

W, solid work function	$2p_{3/2}E_{vacuum}^{solid}$ (eV)[a]	Spectrum in Fig. 3	$2p_{3/2}E_{cl}$ (eV)	ΔE (eV)	Cluster radius (Å)	Number of shells	Estimated cluster size $\langle N\rangle$, atoms
2.75	33.35	Black (large)	33.55	0.20	36	16	$1\times10^4/5\times10^3$
		Gray (small)	33.59	0.24	30	13	$7\times10^3/3\times10^3$
2.95	33.55	Black (large)	33.55	0			
		Gray (small)	33.59	0.04	180	74	$10^6/6\times10^5$

[a]Calculated according to Eq. (3) using E_{solid} from Ref. 15.

Fermi level having zero binding energy. The relationship between these two referencing systems is then given by

$$E_{vacuum} = E_{solid} + W, \tag{3}$$

where W is the binding energy at the Fermi level, e.g., the work function.

From Ref. 15, we find that the binding energy for the lowest bulk $2p_{3/2}$ peak measured relative to the Fermi edge is ≈30.6 eV. The work function is a magnitude known with a rather limited precision. Literature values range from 2.75 to 2.95 eV for Na(110) crystals. For polycrystalline sodium, which the clusters probably belong to, the work function varies in the same range. By considering the limiting values of this range, the corresponding cluster radius can be calculated. From the latter, the number of atoms in a cluster can be obtained using the cluster shell model from Ref. 31 and the intershell separation of 2.48 Å. Another way of estimating the number of atoms per cluster from its dimensions is to use the density of the solid. This approach gives about half as many atoms per cluster as the shell model. The estimated values for the cluster sizes corresponding to the spectra in Fig. 3 are summarized in Table I. Thus, at the smaller size conditions, the size of the clusters estimated from the shell model can be within $\langle N\rangle \approx 7\times10^3-10^6$ atoms, and at the larger size conditions, the size can be from $\langle N\rangle \approx 1\times10^4$ to more than 10^6 atoms. Although the absolute size is not accurately determined, the relative size change is much less affected by the uncertainty in the work function: the size of clusters created at the two discussed clustering conditions differs by a factor of ≈2.

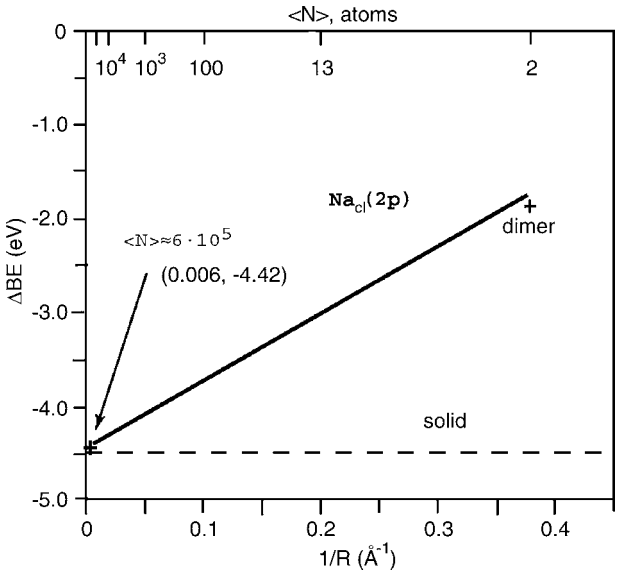

FIG. 6. $2p$ binding-energy difference for Na clusters as a function of $1/R$ and $\langle N\rangle$. The straight line is the graphical presentation of Eq. (1) using the experimental points for $\langle N\rangle = 6\times10^5$ atoms and $E_{cluster}-E_{atom}\approx -4.4$ eV.

Now, it is possible to analyze the electron effective attenuation length for the estimated cluster sizes using the method from Ref. 5. For two kinetic energies in Fig. 3 (≈40 and ≈90 eV), the values of the attenuation length for solid sodium found from Ref. 26 are 5 and 7 Å. As can be seen from Table II a better correspondence to the experimental bulk-to-surface signal ratio is obtained for the larger cluster-size estimate—$\langle N\rangle \approx 10^6$ atoms.

Using Eq. (1) and the absolute binding-energy values for the *large* clusters, we can predict the difference between the cluster and the atom ionization potential as a function of cluster size (Fig. 6). From Eq. (2), this difference should be a linear function of the reciprocal radius or $N^{-1/3}$. The slope of the straight line is predefined by the coefficient at $1/R$, and the other coefficient of the line is given by the experimental point for the clusters.

The large clusters of $\langle N\rangle \approx 10^6$ atoms should resemble solids in many respects. For instance, they should have a formed valence band. The normal Auger spectrum, reflecting the initial-state band structure, should also be similar to the solid case. The next section analyzes the results of the normal Auger measurements.

TABLE II. Bulk-to-surface ratios for the smaller cluster conditions obtained from the experiment (Fig. 3) and from the shell model using the attenuation length (AL) from Ref. 26 for the limit size values.

	I_b/I_s		
Photon energy	Experiment	Shell model	
		$\langle N\rangle \approx 10^4$	$\langle N\rangle \approx 10^6$
74 eV (AL 5 Å)	0.7	0.6	0.7
120 eV (AL 7 Å)	1.0	0.9	1.0

C. Work function and valence-band width from normal Auger spectroscopy

In large Na clusters, the removal of two valence electrons as the result of the Auger decay does not lead to a repulsive state, as it does in Na dimers. The valence band should be well formed by these sizes and is then well described by the free-electron model.[13] The two final-state holes can be regarded, to a great extent, as independent of each other. The spectral shape is then, to the first approximation, given by a self-convolution of the valence-band density of states.[32] The highest kinetic energy Auger electrons are produced when the electron filling the core hole and the Auger electron are ejected from the top of the cluster valence band. This highest energy can be analytically approximated as

$$E_{kin}^{max} = E_b(2p) - \{W_\infty + \Delta W(0)\} - \{W_\infty + \Delta W(+1)\}, \quad (4)$$

where W_∞ is the work function of the planar bulk, $\Delta W(0)$ and $\Delta W(+1)$ are the corrections for the cluster work functions due to the spherical shape and the charge on the cluster, and $E_b(2p)$ is the Na $2p$ binding energies for clusters. For the largest cluster size, the summarized corrections ΔW for ionization energies are $\leqslant$0.2 eV. Taking the 2.95 eV as W_∞ and binding energy $E_b(2p)$=33.5 eV of the $2p_{3/2}$ bulk feature, one gets the $E_{kin}^{max} \approx$ 27.4 eV. Indeed, the experiment gives 27.5 eV measured at half maximum of the Auger feature. This agreement supports the description of the lowest two-hole final state as being due to the removal of two uncorrelated delocalized electrons at the Fermi level.

As it was discussed above in connection to the Doniac-Šunjić XPS line profile, a shake-up-like excitation process due to the core ionization populates the empty conduction band. Further Auger decay can then go either through the so-called participator decay (excited electron fills the core hole) or the spectator decay channels. In the case of the participator decay, the Auger electron kinetic energies would be higher than the E_{kin}^{max} estimated limit, while the experimental value coincides with the E_{kin}^{max}. Hence, the spectatorlike decay seems to dominate.

It is also, in principle, possible to estimate the width of the valence band in a solid from its Auger spectrum. The width of the Auger feature should be approximately two times the width of the filled valence band. From some literature sources,[33,34] the valence-band width $\Delta E_{valence}$ for Na solids is about 3.0 eV, which would result in an approximately 6 eV wide Auger feature. At the same time, the Auger width measured at half maximum in Fig. 6 is $\approx$12 eV. However, there are known differences between the experimentally and theoretically determined bandwidth for Na metal, and the reason for this is still an open issue.[35] The presence of lower kinetic-energy electrons can also be due to the way we probe the valence band. It can be the result of another shake-up-like process taking place during the Auger decay. In the extreme case, when an electron is excited from the valence-band bottom up to the ionization threshold, the Auger electron kinetic energy can be lower than the expected value for $W_\infty + \Delta E_{valence} \approx 2.95 + 3.0 \approx 6$ eV. This can explain the 12 eV width of the experimental Auger feature. One more explanation for the extended width of the Auger feature can be in the Auger electrons which lose a part of their kinetic energy on plasmon excitations, which the energies are up to 6 eV. Summarizing, we can say that the solidlike band energy structure explains well certain aspects of the normal Auger spectrum for large Na clusters. This fact underlines once again that these clusters are nanoscale solids. As for the issue of the Auger feature width, it demands further investigation, both experimental and theoretical.

V. CONCLUSIONS

In conclusion, we have shown that synchrotron-based x-ray core-level photoelectron spectroscopy can be efficiently implemented to free metal clusters. The evolution of electronic structure with size has been studied by XPS and Auger techniques and discussed in comparison with the atom, dimer, and solid. The difference in the established ionization potential of the sodium clusters and of the solid has been used for size estimation of the clusters.

In the XPS, the surface and bulk sites of free metal clusters have been probed effectively by varying the photon energy. These measurements have shown a close similarity of large clusters and solid sodium. The knowledge of Gaussian width of the cluster bulk and surface lines has provided information about the cluster temperature. The estimated cluster temperature has shown that the particles are efficiently thermalized in the source.

The Auger studies have given information on the details of the electronic core-hole state decay and on the valence-band width. The extended Auger spectrum width indicates a strong shake-up process populating the conduction band and possible plasmon excitations.

In general, the results could be well explained using the concepts of solid-state physics. Thus, it underlines that in present experiments, we have created and studied free metallic nanoparticles.

ACKNOWLEDGMENTS

We gratefully acknowledge the financial support of the Knut and Alice Wallenberg Foundation, the Swedish Foundation for Strategic Research, the Goran Gustafsson Foundation, and the Swedish Research Council.

*Electronic address: serguei.peredkov@sljus.lu.se

[1] *Clusters of Atoms and Molecules*, edited by H. Haberland, Springer Series Chemical Physics Vol. 52 (Springer, Berlin, 1994), Vols. I and II.
[2] O. Cheshnovsky, K. J. Taylor, J. Conceicao, and R. E. Smalley, Phys. Rev. Lett. **64**, 1785 (1990).
[3] E. Rühl, C. Heinzel, A. P. Hitchcock, and H. Baumqartel, J. Chem. Phys. **98**, 2653 (1993).
[4] O. Björneholm, F. Federmann, F. Fossing, and T. Moller, Phys. Rev. Lett. **74**, 3017 (1995).
[5] M. Tchaplyguine, R. R. Marinho, M. Gisselbrecht, J. Schulz, N. Mårtensson, S. L. Sorensen, A. Brito, R. Feifel, G. Öhrwall, M. Lundwall *et al.*, J. Chem. Phys. **120**, 345 (2004a).
[6] M. Lundwall, M. Tchaplyguine, G. Öhrwall, R. Feifel, A. Lindblad, A. Lindgren, S. Sorensen, S. Svensson, and O. Björneholm, Chem. Phys. Lett. **392**, 433 (2004).
[7] G. Öhrwall, R. F. Fink, M. Tchaplyguine, L. Ojamäe, M. Lundwall, R. R. T. Marinho, A. Brito, S. L. Sorensen, M. Gisselbrecht, R. Feifel *et al.*, J. Chem. Phys. **123**, 054310 (2005).
[8] T. Hatsui, H. Setoyama, N. Kosugi, B. Wassermann, I. L. Bradeanu, and E. Rühl, J. Chem. Phys. **123**, 154304 (2005).
[9] M. Lundwall, H. Bergersen, A. Lindblad, G. Öhrwall, M. Tchaplyguine, S. Svensson, and O. Björneholm, Phys. Rev. A **74**, 043206 (2006).
[10] M. Tchaplyguine, M. Lundwall, M. Gisselbrecht, G. Öhrwall, R. Feifel, S. Sorensen, S. Svensson, N. Mårtensson, and O. Björneholm, Phys. Rev. A **69**, 031201(R) (2004).
[11] S. L. Qiu, X. Pan, M. Strongin, and P. H. Citrin, Phys. Rev. B **36**, 1292 (1987).
[12] P. Piseri, T. Mazza, G. Bongiorno, C. Lenardi, L. Ravagnan, F. Foglia, F. DiFonzo, M. Coreno, M. DeSimone, K. C. Prince *et al.*, New J. Phys. **8**, 136 (2006).
[13] G. Wrigge, M. Astruc Hoffmann, and B. Issendorff, Phys. Rev. A **65**, 063201 (2002).
[14] J. Schulz, M. Tchaplyguine, T. Rander, O. Björneholm, S. Svensson, R. Sankari, S. Heinäsmäki, H. Aksela, S. Aksela, and E. Kukk, Phys. Rev. A **72**, 010702(R) (2005).
[15] D. M. Riffe, G. K. Wertheim, and P. H. Citrin, Phys. Rev. Lett. **67**, 116 (1991).
[16] T. Rander, J. Schulz, M. Huttula, A. Mäkinen, M. Tchaplyguine, S. Svensson, G. Öhrwall, O. Björneholm, S. Aksela, and H. Aksela, Phys. Rev. A **75**, 032510 (2007).
[17] G. K. Wertheim, D. M. Riffe, and P. H. Citrin, Phys. Rev. B **45**, 8703 (1992a).
[18] U. Zimmermann, N. Malinowski, U. Näher, S. Frank, and T. P. Martin, Z. Phys. D: At., Mol. Clusters **31**, 85 (1994).
[19] C. Ellert, M. Schmidt, C. Schmitt, T. Reiners, and H. Haberland, Phys. Rev. Lett. **75**, 1731 (1995).
[20] K. Wong, G. Tikhonov, and V. V. Kresin, Phys. Rev. B **66**, 125401 (2002).
[21] M. Tchaplyguine, S. Peredkov, H. Svensson, J. Schulz, G. Öhrwall, M. Lundwall, T. Rander, A. Lindblad, H. Bergersen, S. Svensson *et al.*, Rev. Sci. Instrum. **77**, 033106 (2006).
[22] M. Bässler, A. Ausmees, M. Jurvansuu, R. Feifel, J.-O. Forsell, P. de Tarso Fonseca, A. Kivimäki, S. Sundin, S. L. Sorensen, R. Nyholm *et al.*, Nucl. Instrum. Methods Phys. Res. A **469**, 382 (2001).
[23] A. Kikas, S. J. Osborne, A. Ausmees, S. Svensson, O.-P. Sairanen, and S. Aksela, J. Electron Spectrosc. Relat. Phenom. **77**, 241 (1996).
[24] S. Doniach and M. Sunjic, J. Phys. C **2**, 285 (1970).
[25] H. Bergersen, M. Abu-samha, J. Harnes, O. Björneholm, S. Svensson, L. J. Sæthre, and K. J. Børve, Phys. Chem. Chem. Phys. **8**, 1899 (2006).
[26] G. K. Wertheim, D. M. Riffe, N. V. Smith, and P. H. Citrin, Phys. Rev. B **46**, 1955 (1992).
[27] F. G. Amar, J. Smaby, and T. J. Preston, J. Chem. Phys. **122**, 244717 (2005).
[28] M. A. Hoffmann, G. Wrigge, and B. V. Issendorff, Phys. Rev. B **66**, 041404(R) (2002).
[29] G. Makov and A. Nitzan, J. Chem. Phys. **88**, 5076 (2002).
[30] K. Rademann, O. Dimopoulou-Rademann, M. Schlauf, U. Even, and F. Hensel, Phys. Rev. Lett. **69**, 3208 (1992).
[31] R. E. Benfield, J. Chem. Soc., Faraday Trans. **88**, 1107 (1992).
[32] G. A. Sawatzky, Phys. Rev. Lett. **39**, 504 (1977).
[33] H. Höchst, P. Steiner, and S. Hüfner, Z. Phys. B **30**, 145 (1978).
[34] S. Prutzer and S. M. Bose, Phys. Rev. B **31**, 762 (1985).
[35] H. Yasuhara, S. Yoshinaga, and M. Higuchi, Phys. Rev. Lett. **83**, 3250 (1999).